Available online at www.sciencedirect.com
ScienceDirect
Fusion Engineering and Design 82 (2007) 1144–1152
Fusion Engineering and Design
www.elsevier.com/locate/fusengdes

Equilibrium reconstruction improvement via Kalman-filter-based vessel current estimation at DIII-D

Y. Ou [a], M.L. Walker [b], E. Schuster [a,*], J.R. Ferron [b]

[a] *Department of Mechanical Engineering and Mechanics, Lehigh University, Bethlehem, PA, USA*
[b] *General Atomics, San Diego, CA, USA*

Received 25 September 2006; received in revised form 12 April 2007; accepted 13 April 2007
Available online 11 June 2007

Abstract

Equilibrium reconstruction codes calculate the distributions of flux and toroidal current density over the plasma and surrounding vacuum region that best fit the external magnetic measurements in a least square sense, and that simultaneously satisfy the MHD equilibrium equation (Grad-Shafranov equation). Although these codes often use direct measurements of the currents in the plasma and poloidal coils, they sometimes neglect the current induced in the tokamak vessel due to the fact that they cannot be directly measured. Kalman filtering theory is employed in this work to optimally estimate the current in the tokamak vessel. The real-time version of the EFIT code is modified to accept the estimated vessel currents with the goal of improving the equilibrium reconstruction for the DIII-D tokamak.

Keywords: Equilibrium reconstruction; Optimal estimation; Vessel currents

1. Introduction

The efficient and safe operation of fusion devices relies on accurate knowledge of many of the discharge parameters. The values of several discharge parameters which are not directly measurable, such as plasma shape and current density distribution, can be reconstructed from magnetic field and flux measurements. Equilibrium codes, such as EFIT [1], calculate the distributions of flux and toroidal current density over the plasma and surrounding vacuum region that best fit, in a least square sense, the external magnetic measurements, and that simultaneously satisfy the MHD equilibrium equation (Grad-Shafranov equation) [2]. Once the flux distribution is known, it is possible to reconstruct the plasma boundary for shape control purposes.

The most general treatment of toroidal current sources in the fitting problem assumes that they are

* Corresponding author.
E-mail address: schuster@lehigh.edu (E. Schuster).

0920-3796/$ – see front matter © 2007 Elsevier B.V. All rights reserved.
doi:10.1016/j.fusengdes.2007.04.030

all unknown. Thus, in addition to the plasma toroidal current, the currents in the poloidal field (PF) coils can be free parameters and, potentially, the induced currents in the vacuum vessel and support structures can be treated this way as well. There are direct measurements of the PF coil currents, but these measurements have uncertainties which can be properly accounted for in the least squares fitting procedure by solving for the external currents using the measurements as constraints. A similar procedure could be followed for the vessel currents if they were measurable. Unfortunately, this is not usually the case.

Kalman filtering theory is used in this work to optimally estimate the current in the tokamak vessel. With the ultimate goal of improving the equilibrium reconstruction for the DIII-D tokamak, the real-time version of the EFIT algorithm [3] is modified to accept the estimated vessel currents. Furthermore, it will be shown that the integration of Kalman filter estimation into the equilibrium reconstruction algorithm provides a new way to validate and refine the plasma dynamic model. The important effect of vessel or structure currents has been recognized in many plasma control applications [3,4]. Prior work on the incorporation of an electromagnetic model of the passive structures in the identification of the plasma magnetic boundary, but without including any MHD equilibrium model, can be found in [5,6]. Some previous effort on incorporating an estimate of the vessel current into the equilibrium reconstruction algorithm has been done at NSTX [7]. Estimated values for the resistances in each one of the vessel segments are used to compute the currents for each vessel segment, given the measured loop voltages. However, since the discrete loop voltage sensors do not identically reproduce the voltage over the vessel segments, the computed vessel currents suffer from relatively large errors. The Kalman filter is a refinement on the NSTX approach which provides additional physics for improving the exactness of the fit, once all the competing physics constraints have been reconciled.

This paper is organized as follows. In Section 2, the basis of equilibrium reconstruction is discussed. Section 3 describes the Kalman-filter-based optimal estimation approach for the vessel currents, and introduces the linearized dynamic model of the plasma. How to integrate the estimated vessel currents into the real-time equilibrium reconstruction algorithm is addressed in Section 4. Section 5 presents some present results. Finally, conclusions and identified future work are presented in Section 6.

2. Equilibrium reconstruction basis

The primary objective of equilibrium reconstruction is twofold: (1) substantially improve the accuracy with which the plasma boundary is estimated, thereby improving control, (2) obtain reliable (consistent both with known physics and with available measurements) estimates of internal parameters, such as the current profile.

Assuming an axisymmetric plasma in a cylindrical coordinate system $\{r, \phi, z\}$, the equilibrium MHD equations (fluid mechanics equations + Maxwell's equations) reduce to the Grad-Shafranov equation:

$$\Delta^* \psi_{\mathrm{p}} = -\mu_0 r J_\phi \tag{1}$$

which describes the force balance of the tokamak equilibrium. The elliptic operator Δ^* is given by $\Delta^*\psi = \partial^2\psi/\partial z^2 + r(\partial/\partial r)((1/r)(\partial\psi/\partial r))$, J_ϕ is the toroidal component of the current density, and $\psi = \psi_{\mathrm{p}} + \psi_{\mathrm{ext}}$ is the total poloidal flux per radian, i.e., $\psi = \psi_{\mathrm{pol}}/2\pi$, where ψ_{p} is the poloidal flux resulting from the plasma current and ψ_{ext} is the poloidal flux generated by current in the sources external to the plasma, like coil and induced current.

The task of the equilibrium reconstruction is to calculate the distributions in the r, z plane of the poloidal flux ψ, and the toroidal current density J_ϕ, that provide a least squares best fit to the diagnostic data and which simultaneously satisfy the Grad-Shafranov Eq. (1). The solution to the equilibrium reconstruction problem is obtained through an iterative algorithm that estimates the magnetic measurement C^{m+1} using the flux ψ^m in the plasma domain Ω^m calculated in the previous step m. The magnetic measurements usually have two contributions, one due to the external conductor currents I_{e}, and the other due to the plasma current J_ϕ. The magnetic measurement C at a generic point Z_j is obtained from the current sources placed at locations Z_i's by means of Green's functions G [8]:

$$C_{Z_j}^{m+1} = \sum_{i=1}^{N_{\mathrm{c}}} G(Z_j, Z_i) I_{\mathrm{e}_i} + \int\int_{\Omega^m} G(Z_j, Z) J_\phi(Z, \psi^m)\, \mathrm{d}Z \tag{2}$$

The estimated magnetic measurements C's generated by EFIT, at certain locations where magnetic sensors are placed, are compared with data from those magnetic sensors, to obtain the plasma current $J_\phi^{m+1}(\psi^m)$ that minimizes the quadratic error:

$$\chi^2 = \sum_{k=1}^{N_{\text{meas}}} \left(\frac{M_k - C_k}{\sigma_k} \right)^2 \tag{3}$$

where M_k, C_k, and σ_k are the measured values, the computed values, and the error associated with the k measurement. The flux function is finally updated solving the Grad-Shafranov Eq. (1):

$$\Delta^* \psi^{m+1} = -\mu_0 r J_\phi^{m+1}(\psi^m) \tag{4}$$

The real-time version of EFIT [3] uses a two-loop scheme. A fast loop performs the least squares fit (3) using new measured values from the magnetic sensors in each iteration but using the last equilibrium flux provided by the solution of (4). The plasma current J_ϕ in each iteration is used to compute, through Green's functions, the magnetic flux values at a predefined set of control points (geometrical points at which the poloidal magnetic flux is regulated by the shape controller). A slow loop, approximately 25 times slower than the fast loop, solves the equilibrium problem (4) to update the magnetic flux ψ.

In real-time EFIT [3], the diagnostic data presently consist of measurements of magnetic flux and field outside the plasma, plasma plus vessel current from a Rogowskii loop, field internal to the plasma from a motional stark effect diagnostic, and current in the poloidal field and ohmic heating coils. One of the main contributions of this work is the incorporation of estimated induced vessel currents into the diagnostic data set (Section 4).

3. Vessel current estimation

The system composed of plasma, shaping coils, and passive structure can be described using circuit equations derived from Faraday's law, and radial and vertical force balance relations for a particular plasma equilibrium. In addition, rigid radial and vertical displacement of the equilibrium current distribution is assumed, and a resistive plasma circuit equation is specified. The result is a circuit equation describing the linearized response, around a particular plasma equilibrium, of the conductor–plasma system to voltages applied to active conductors. The model equations for poloidal field (PF) coil current, vessel (passive conductor) currents, and plasma current are respectively:

$$\begin{aligned} M^*_{\text{cc}}\dot{I}_{\text{c}} + R_{\text{c}} I_{\text{c}} + M^*_{\text{cv}}\dot{I}_{\text{v}} + M^*_{\text{cp}}\dot{I}_{\text{p}} &= V_{\text{c}} \\ M^*_{\text{vv}}\dot{I}_{\text{v}} + R_{\text{v}} I_{\text{v}} + M^*_{\text{vc}}\dot{I}_{\text{c}} + M^*_{\text{vp}}\dot{I}_{\text{p}} &= 0 \\ M^*_{\text{pp}}\dot{I}_{\text{p}} + R_{\text{p}} I_{\text{p}} + M^*_{\text{pc}}\dot{I}_{\text{c}} + M^*_{\text{pv}}\dot{I}_{\text{v}} &= V_{\text{no}} \end{aligned} \tag{5}$$

where I_{c}, I_{v}, and I_{p} represent currents in PF coils, vessel, and plasma, respectively. V_{c} the vector of voltages applied to the PF coils, and V_{no} is the effective voltage applied to drive plasma current by noninductive sources. R_{a}, for $\text{a} \in \{\text{c, v, p}\}$, represents the resistance matrix of each one of the circuits. $M^*_{\text{ab}} = M_{\text{ab}} + X_{\text{ab}}$ are plasma-modified mutual inductance, where $\text{a, b} \in \{\text{c, v, p}\}$. M_{ab} is the usual conductor-to-conductor mutual inductance, and X_{ab} describes a plasma motion-mediated inductance, linearized around the plasma equilibrium. The plasma response matrix X_{ab}, representing changes in flux due to plasma motion, are functions only of the equilibrium current distribution and vacuum magnetic field B_{eq}. The X_{ab} matrix is computed starting with an EFIT equilibrium [1], and added to the mutual inductance M_{ab} as part of the model construction process.

In contrast to the dynamic Eq. (5), the mapping from currents to outputs (for example, diagnostic data such as flux loops, magnetic probes, Rogowskii loops) is expressed explicitly in terms of current deviations from equilibrium values [9]:

$$\delta y = C_{I_{\text{c}}} \delta I_{\text{c}} + C_{I_{\text{v}}} \delta I_{\text{v}} + C_{I_{\text{p}}} \delta I_{\text{p}} \tag{6}$$

where $\delta T = T - T_{\text{eq}}$, for $T \in \{I_{\text{c}}, I_{\text{v}}, I_{\text{p}}, y\}$. The subscript "eq" denotes values at the equilibrium from which the models (5) and (6) are derived. In the rest of the paper, δ will be omitted for simplicity, but it will be implicitly assumed that the output equation is written in terms of deviation variables. The matrices $C_{I_{\text{s}}}$, for $I_{\text{s}} \in \{I_{\text{c}}, I_{\text{v}}, I_{\text{p}}\}$, are defined as

$$C_{I_{\text{s}}} = \frac{\partial y}{\partial I_{\text{s}}} + \frac{\partial y}{\partial r_{\text{c}}} \frac{\partial r_{\text{c}}}{\partial I_{\text{s}}} + \frac{\partial y}{\partial z_{\text{c}}} \frac{\partial z_{\text{c}}}{\partial I_{\text{s}}} \tag{7}$$

where the first term on the right hand side is the "direct" response, e.g., given by Green's function calculations in the case of magnetic probes or flux loops. The remaining terms are responses due to motion of the

plasma; r_c and z_c denote the radial and vertical positions of the plasma current centroid, i.e., "center of mass" of the current. It is common to include disturbance terms describing the response to variations in kinetic and current profile quantities such as poloidal beta (β_p), and normalized internal inductance (ℓ_i) [10]. However, disturbance terms are neglected in the present study.

If the estimation of the vessel current is the only objective, a simplified model for the dynamics of the vessel current can be extracted from (5). The second equation in (5), combined with (6), can be rewritten in state space form as

$$\begin{aligned} \dot{x}_v &= A_v x_v + B_v u_v + G_v w_1 \\ y &= C_v x_v + D_v u_v + w_2 \end{aligned} \tag{8}$$

where $x_v = I_v$, $u_v = [I_c^T \;\; I_p^T \;\; \dot{I}_c^T \;\; \dot{I}_p^T]^T$. The new system matrices are $A_v = -M_{vv}^{*\,-1} R_v$, $B_v = -M_{vv}^{*\,-1}[0 \;\; 0 \;\; M_{vc}^* \;\; M_{vp}^*]$, $G_v = B_v$, $C_v = C_{I_v}$, $D_v = [C_{I_c} \;\; C_{I_p} \;\; 0 \;\; 0]$. The output y may include flux loops, magnetic probes, and Rogowskii loops. Process noise or disturbance w_1, and measurement noise w_2 has been added to the model (8). The noise covariance matrices are given by $\varepsilon\{w_1 w_1^T\} = Q_n$, $\varepsilon\{w_2 w_2^T\} = R_n$. To optimally estimate the vessel current I_v, we implement a Kalman filter [11]:

$$\dot{\hat{x}}_v = A_v \hat{x}_v + B_v u_v + K(y - C_v \hat{x}_v - D_v u_v) \tag{9}$$

where $\hat{x}_v$ is the estimation for x_v. Solving the Riccati equation for Y:

$$0 = A_v Y + Y A_v^T + G_v Q_n G_v^T - Y C_v^T R_n^{-1} C_v Y,$$

we can obtain the Kalman gain matrix $K = Y C_v^T R_n^{-1}$. Carefully tuning Q_n and R_n, based on the knowledge of the system, an optimal estimation of the vessel current can be obtained.

4. Reconstruction with vessel currents

The equilibrium solution consists of values of ψ and J_ϕ on a rectangular grid which covers the entire area of the vacuum vessel. The current is modeled as being distributed among a set of rectangular elements, one centered at each grid point, with the total number of grid points typically 1000 or more. The large number of grid points allows the solution to provide a realistic distribution of the current density, including provision for finite current density at the discharge edge. In the Grad-Shafranov Eq. (1), the toroidal current density J_ϕ is written as

$$J_\phi = r\left(\frac{\partial P}{\partial \psi} + \frac{\mu_0 F}{4\pi^2 r^2}\frac{\partial F}{\partial \psi}\right) \tag{10}$$

where P is the plasma pressure, and the auxiliary function F is proportional to the poloidal current $I_{pol} = 2\pi F/\mu_0$ flowing in the plasma. Although J_ϕ is modeled as being distributed among a large set of rectangular elements, it is parameterized by only a small number of free parameters. Simple polynomial models are used to represent P' and FF':

$$\frac{\partial P}{\partial \psi} = \sum_{n=0}^{n_p} \alpha_n \left[\psi_N + \frac{\partial \psi_N}{\partial z}\delta z\right]^n \tag{11}$$

$$\frac{\mu_0 F}{4\pi^2}\frac{\partial F}{\partial \psi} = \sum_{n=0}^{n_F} \gamma_n \left[\psi_N + \frac{\partial \psi_N}{\partial z}\delta z\right]^n \tag{12}$$

where $\alpha_\mathbf{J} = [\alpha_0, \alpha_1, \ldots, \alpha_{n_p}]$, $\gamma_\mathbf{J} = [\gamma_0, \gamma_1, \ldots, \gamma_{n_F}]$, and δz are the free parameters. The free parameter δz allows the equilibrium reconstruction to follow the vertical movement of the discharge. Of the terms containing δz, only those linear in δz are retained in (11) and (12). We define $\Theta = [\alpha_\mathbf{J}, \gamma_\mathbf{J}, \delta z]$ as the set of free parameters in the parameterizations of J_ϕ. The normalized flux is defined as $\psi_N = (\psi - \psi_c)/(\psi_b - \psi_c)$, where ψ_c is the poloidal flux at the magnetic axis (center of the nested magnetic flux surfaces), and ψ_b is the poloidal flux at the plasma boundary. The normalized flux ψ_N provides an adjustable mapping from the small number of fitting parameters to the large number of grid points on the r, z plane. The discretized plasma current model is written as [3]:

$$I_\phi = \Psi \times \Theta \tag{13}$$

where there is one row in the matrix Ψ for each grid element and the column values are the coefficients of elements of $\alpha_\mathbf{J}$ and $\gamma_\mathbf{J}$ from Eqs. (11) and (12). The ith row of the matrix Ψ is given by

$$\Psi_i = \left[r_i, r_i\psi_{N_i}, \ldots, r_i\psi_{N_i}^{n_p}, \frac{1}{r_i}, \frac{\psi_{N_i}}{r_i}, \ldots, \frac{\psi_{N_i}^{n_F}}{r_i}, C_{\delta z_i}\right] \tag{14}$$

where the subindex i denotes that the quantities are evaluated at the ith grid point. All terms linearly proportional to δz are collected into $C_{\delta z}$. In addition to the plasma toroidal current, the currents in the external poloidal field (PF) coils, I_c, have been considered so far as free parameters. The direct measurements of the external PF coil currents have uncertainties that are properly accounted for in the least squares fitting procedure by solving for the external currents using the available measurements as constraints. The DIII-D flux loops are wired so that all flux measurements are made relative to the total flux measured at a single reference position. This reference flux value (ψ_{ref}) has also been treated then as a free parameter with the measured value weighted by its uncertainty used as a constraint. In this work, we add the vessel current to the set of free parameter. With this purpose, the vessel structure has been discretized into 28 segments as it is shown in Fig. 1 (a). The 28 vessel currents, I_v, are considered as free parameters in the fitting procedure. The optimal vessel current estimations, provided by the Kalman filter implementation, are incorporated as an additional constraints after weighting them by their uncertainties. Thus, the total vector of unknowns for the fitting problem is now $U = [I_c, I_v, \Theta, \psi_{ref}]$.

Considering the discretization of the toroidal current (13) and including the discretized vessel currents, (2) can be rewritten in matrix form as

$$C = \zeta \times U \tag{15}$$

The diagram in Fig. 2 shows the response matrix ζ. Blocks (a) and (b) in the matrix contain the precalculated Green's function coefficients that specify the contribution to the magnetic measurement C by each of the external coil currents and induced vessel currents. Block (c) represents the contribution to the magnetic measurement C by the plasma current at each grid element. When the magnetic measurements are calculated at positions where magnetic diagnostics are placed,

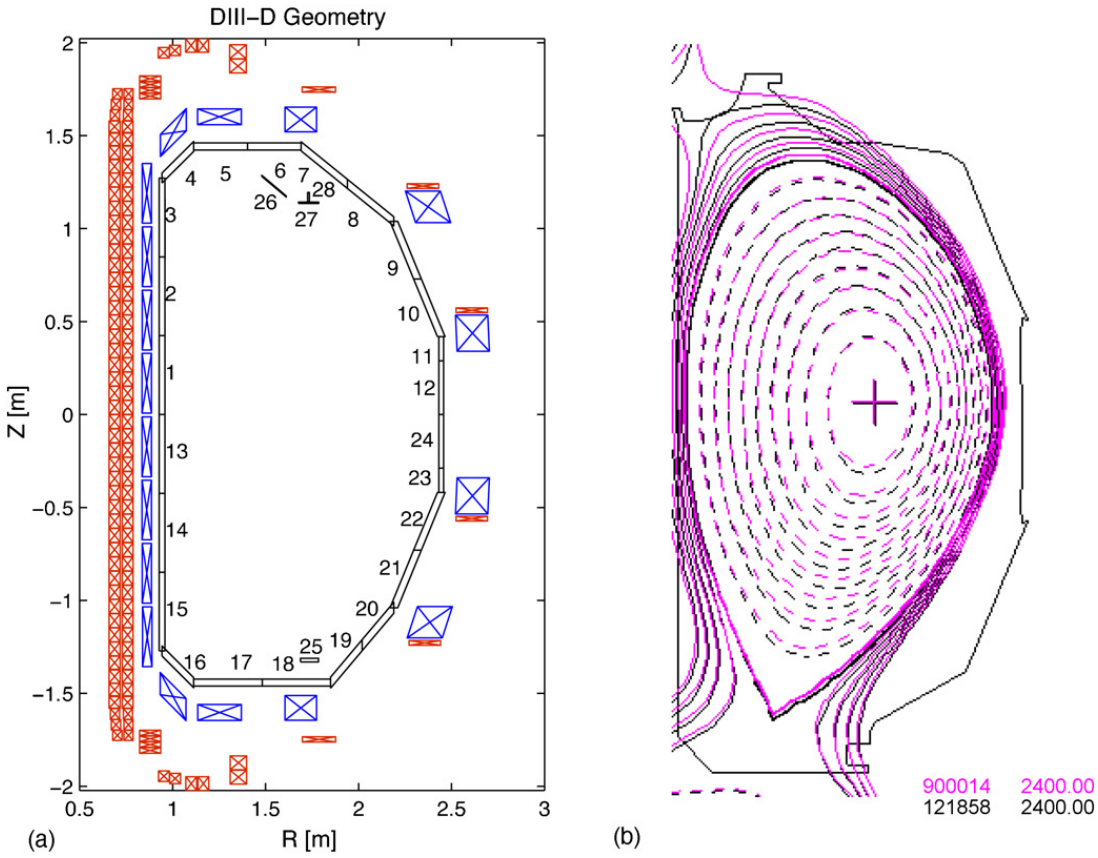

Fig. 1. (a) Cross-section of discretized vessel model and (b) discharge shape comparison (shots 121858, 900014) at 2400 ms.

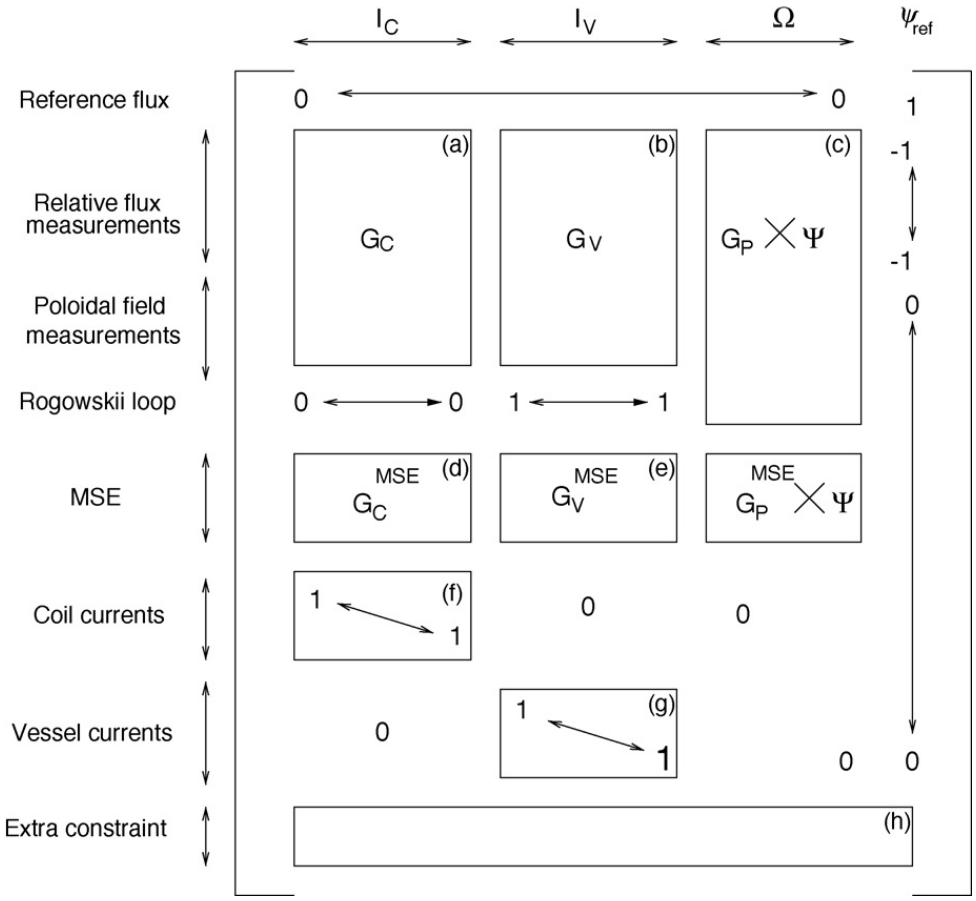

Fig. 2. Schematic of the matrix ζ that relates D to U.

we are interested in finding the vector U that makes these measurements equal to the values measured by the sensors, i.e., the diagnostic data D. Therefore, (15) is rewritten as

$$D = \zeta \times U \tag{16}$$

Because the number of diagnostic measurements is usually much larger than the number of fitting parameters, (16) is not an exact relation. This leads to the requirement that U be obtained in a least squares sense. After multiplying both sides of (16) by a weight vector W, that has one element for each diagnostic signal equal to the inverse of the measurement uncertainty (or estimation uncertainty, in the case of the vessel currents). The solution that minimizes (3) is obtained by using the pseudo-inverse of the weighted response matrix, i.e.,

$$U = (W \cdot \zeta)^{-1} \times (W \cdot D) \tag{17}$$

where the operator "$\cdot$" indicates multiplication of each column of the matrix by the vector, and the operator "$\times$" indicates matrix multiplication. The vector of all the axisymmetric current sources, $I_{\mathrm{axi}} = [I_{\mathrm{c}}, I_{\mathrm{v}}, I_{\phi}]$, is assembled from the solution for U. The flux is updated by solving (4), which ensures the fulfillment of the Grad-Shafranov equation.

5. Results

We use a data set from experimental discharges at DIII-D to study the effectiveness of the Kalman filter (9) in estimating the induced vessel currents. In all the cases presented in this section, we consider that the output vector of the system (8) is composed only of magnetic flux loops and Rogowskii loops.

We estimate the vessel current in the interval 1.5–4.0 s. for DIII-D experimental discharge (shot)

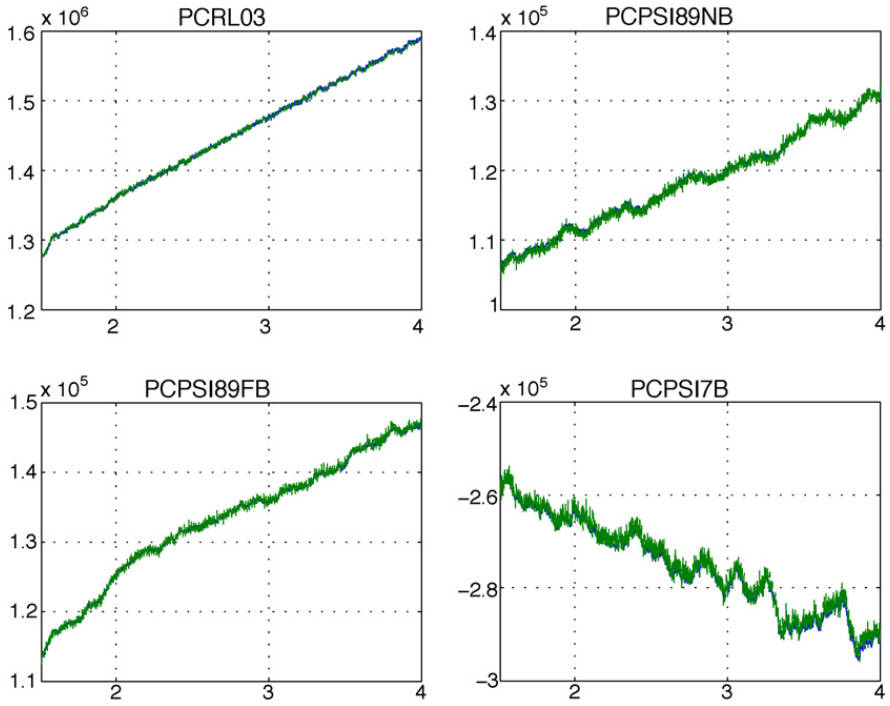

Fig. 3. Kalman filter estimation for shot 118572 (time (horizontal axis) [s], magnetic flux [Wb], current [A]). (For interpretation of the references to color in this figure legend, the reader is referred to the web version of the article.)

118572, which corresponds to an approximate flattop stage of the plasma current evolution. By carefully tuning Q_n and R_n, the output of the Kalman filter matches the diagnostic data. Fig 3 shows the results for some of the output variables; "PCRL03" is one of the Rogowskii loops, and "PCPSI89NB", "PCPSI89FB" and "PCPSI7B" are three of the magnetic flux loops. The figure compares measured (blue) and Kalman-filter-estimated (green) values. Due to the good matching it is difficult to distinguish both signals from the figure.

Present models used by the equilibrium reconstruction algorithm and the Kalman filter are not totally consistent, in particular for the inner vessel segments (segments 1, 2, 3, 13, 14, 15 in Fig. 1 (a)). For this reason, we set weights (matrix W in (17)) for these vessel segments that are 1000 times smaller than those for the other vessel segments.

We compare now reconstruction results for the time interval 2.0–3.0 s, with and without using the vessel current estimates. The reconstruction results obtained using the estimates of the vessel currents are stored in the virtual shot 900014, while those obtained without using the vessel currents estimates are simply labeled 121858. Table 1 compares the resulting χ^2 at $t = 2400$ ms for both shots. The PF coil χ^2 contains vessel current errors as well as coil current errors for 900014. We can appreciate that χ^2 is indeed reduced by incorporating the currents of the vessel segments as free parameters. The similarities between the vessel currents estimated by the Kalman filter and the real-time EFIT, shown in Fig. 4, suggest that the fitting error is minimized at a physical solution. Thus, the equilibrium reconstruction has been improved. The flux surfaces and plasma boundary for both shots are compared in Fig. 1 (b). We expect this similarity for equilibria in plasma current flattop, since vessel currents are relatively small at those times. The goal is to validate the method with these comparisons, then apply

Table 1
χ^2 comparison for shots 121858 and 900014 at 2400 ms

Shot	PF-coil	B-probe	Flux loops	Total
121858	1.98	33.23	5.34	40.496
900014	5.06	17.42	2.44	25.103

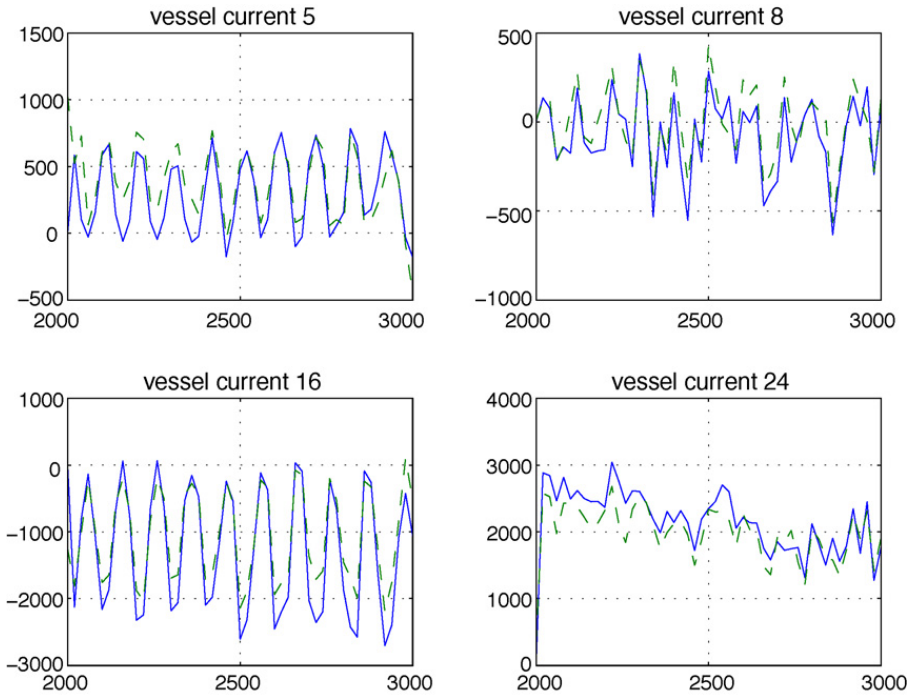

Fig. 4. Kalman-filter-estimated I_v (green dashed) and real-time EFIT computed I_v (blue solid) (time (horizontal axis) [ms], currents [A]). (For interpretation of the references to color in this figure legend, the reader is referred to the web version of the article.)

the method to situations where large and changing vessel currents are expected, such as in plasma current rampup or rampdown.

6. Conclusions

The proposed Kalman filter solution improves on the physics model used for the fit by adding free parameters representing currents flowing in the vessel conductors. This approach also provides additional physics, defined by the dynamics of the current evolution, that constrain the currents that flow in these conductors. Further work is needed to correctly incorporate estimation uncertainty (analogous to measurement uncertainty) to balance the effect of free parameters and constraints. The advantages of the Kalman filter estimated currents are that they provide current estimates to the reconstruction with substantially reduced noise levels and at the same time are able to track fast changes in vessel currents.

For the inner vessel segments, the currents estimated by the Kalman filter and the real-time EFIT show considerable disagreements. Using the vessel currents estimated by EFIT as the output of the dynamic model (8), a system identification approach can be followed to better estimate the uncertain parameters in the dynamic model such as the resistances of the vessel segments. Kalman filter theory arises as a powerful tool for model reconciliation, which is a very common, and at the same time difficult, problem in plasma physics.

Future work includes the development of a scheduling rule to update the linearized plasma model used by the Kalman filter as the equilibrium evolves.

Acknowledgement

This work was supported in part by a grant from the Commonwealth of Pennsylvania, Department of Community and Economic Development, through the Pennsylvania Infrastructure Technology Alliance (PITA), the NSF CAREER award program (ECCS-0645086), and DoE contract number DE-FC02-04ER54698.

References

[1] L.L. Lao, H. St. John, R.D. Stambaugh, A.G. Kellman, W. Pfeiffer, Reconstruction of current profile parameters and plasma shapes in tokamaks, Nucl. Fusion 25 (1985) 1611–1622.

[2] J.P. Freidberg, Ideal Magnetohydrodynamics, Plenum Press, New York, 1987.
[3] J.R. Ferron, M.L. Walker, L.L. Lao, H.E.S. John, D.A. Humphreys, J.A. Leuer, Real time equilibrium reconstruction for tokamak discharge control, Nucl. Fusion 38 (1998) 1055–1066.
[4] G. Ambrosino, R. Albanese, Magnetic control of plasma current, position, and shape in tokamaks: a survey on modeling and control approaches, IEEE Control Syst. Mag. 25 (2005) 76–92.
[5] A. Stella, F. Trevisan, A method for the identification of the plasma magnetic boundary in machines for fusion research, IEEE Trans. Magn. 36 (4) (2000) 780–784.
[6] P. Bettini, F. Trevisan, A. Formisano, An approach to the plasma magnetic contour identification in presence of eddy currents, IEEE Trans. Magn. 38 (2) (2002) 1089–1092.
[7] S.A. Sabbagh, S.M. Kaye, J. Menard, F. Paoletti, M. Bell, R.E. Bell, et al., Equilibrium properties of spherical torus plasmas in NSTX, Nucl. Fusion 41 (2001) 1601.
[8] E.W. Weisstein, Green's function, in: *MathWorld* —A Wolfram Web Resource, 1999 (http://mathworld.wolfram.com/GreensFunction.html).
[9] M.L. Walker, D.A. Humphreys, Valid coordinate systems for linearized plasma shape response models in tokamaks, General Atomics Report GA-A25042, 2005.
[10] D.A. Humphreys, J.A. Leuer, M.L. Walker, Minimal plasma response models for design of tokamak equilibrium controllers with high dynamic accuracy, Bull. Am. Phys. Soc. 44 (1999) 175–182.
[11] A. Gelb (Ed.), Applied Optimal Estimation, M.I.T. Press, Cambridge, Massachusetts, 1989.